Spring 5-1-2012

# Synthesis and Structural Studies of Calcium and Magnesium Diphosphonate Compounds

Seungmo Suh

Follow this and additional works at: https://surface.syr.edu/honors_capstone
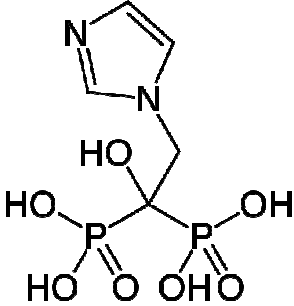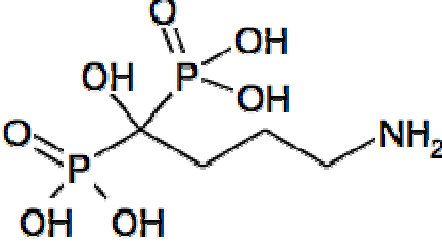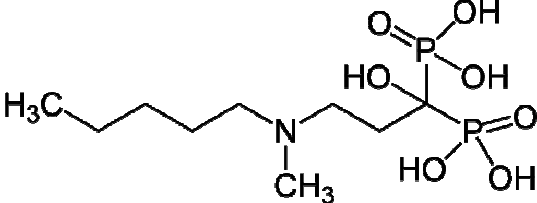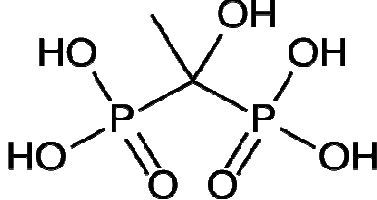
Part of the Biochemistry Commons

**Chapter 1: Background**

**1.1 Introduction**

The chemistry of transition metal phosphonates has enormous potential and diverse applications such as gas separation, gas storage or catalyst systems which have been explored in detail.[1-6] In contrast, analogous chemistry with the *s*-block elements has received only a little attention. Calcium was the priority element in our study due to its bioactive properties. Previous studies proved that phosphonates can possibly be used as bone repair materials.[1] The possible applications are only possible with structures with pores or channels for other molecules to enter. Thus, the control of the shape and size of pores or channels are significant for its applications.[7]

The use of phosphonates and diphosphonates are widely used because they have shown significant therapeutic features for bone related diseases.[8,9] While exogenous phosphonic acids are known to bind to calcium in the bone, diphosphonates are known as agents for suppressing resorption of bone.[10,11] Thus, commonly used diphosphonic acid based drugs are Zoledronate, Alendronate, Ibandronate, and Etidronate and is shown in Table 1.[12] These drugs are used in clinics to treat bone disorders such as osteoporosis, bone metastases, hypercalcemia and Paget's disease. They also cause significant increase in bone mass and decrease in fracture rates by 50%.[13]

Table 1. List of known drugs for treating bone diseases.

| Compound Name | Structure | Brand Name(s) |
|---|---|---|
| Zoledrinic acid |  | Reclast<br><br>Zometa<br><br>Zomera<br><br>Aclasta |
| Alendronic acid |  | Fosamax |
| Ibandronic acid |  | Bonvia<br><br>Bondronate<br><br>Bonviva |
| Etidronic acid |  | Didronel |

The use of diphosphonic acid based drugs is possibly due to their similarity to hydroxyapatite, an important substance in skeletal system, and their resistance to chemical breakdown or hydrolysis.[14]

Furthermore, the potential use of phosphonates and diphosphonates as biomimetric substances is extended by the successful use of mono and

diphosphonates to destroy a variety of protozoa and parasites which are responsible for diseases such as malaria and sleeping sickness (African trypanosomiasis).[15,16] Another significant use of diphosphonates is in water softener (Calgon) to prevent scaling.[17]

## 1.2 Aims and objectives

This project is geared to gain synthetic access to magnesium and calcium phosphonates, to develop synthetic methodologies, and obtain an understanding of structure determining factors in the process of MOFs. The project consists of the preparation of ligand, 3-oxapentane-1,5-diphosphonic acid and metal complexes with the ligand. In addition, it consists of optimization of crystal growth conditions, and structural analysis by single crystal X-ray diffraction.

## 1.3 Literature review
## 1.3.1 Bone material

The skeletal system is the body system that consists of bone, cartilage, tendons, and ligaments. The known functions of the skeletal system are support, protection, movement, blood production, and bone marrow storage.[18,19] The rigid characteristic of the bones allows them to be the most suitable for supporting tissue of the body and providing support. Bones are often found in different cavities in our body system protecting organs such as the brain. The detailed structure of bones is shown in Figure 1.[20]
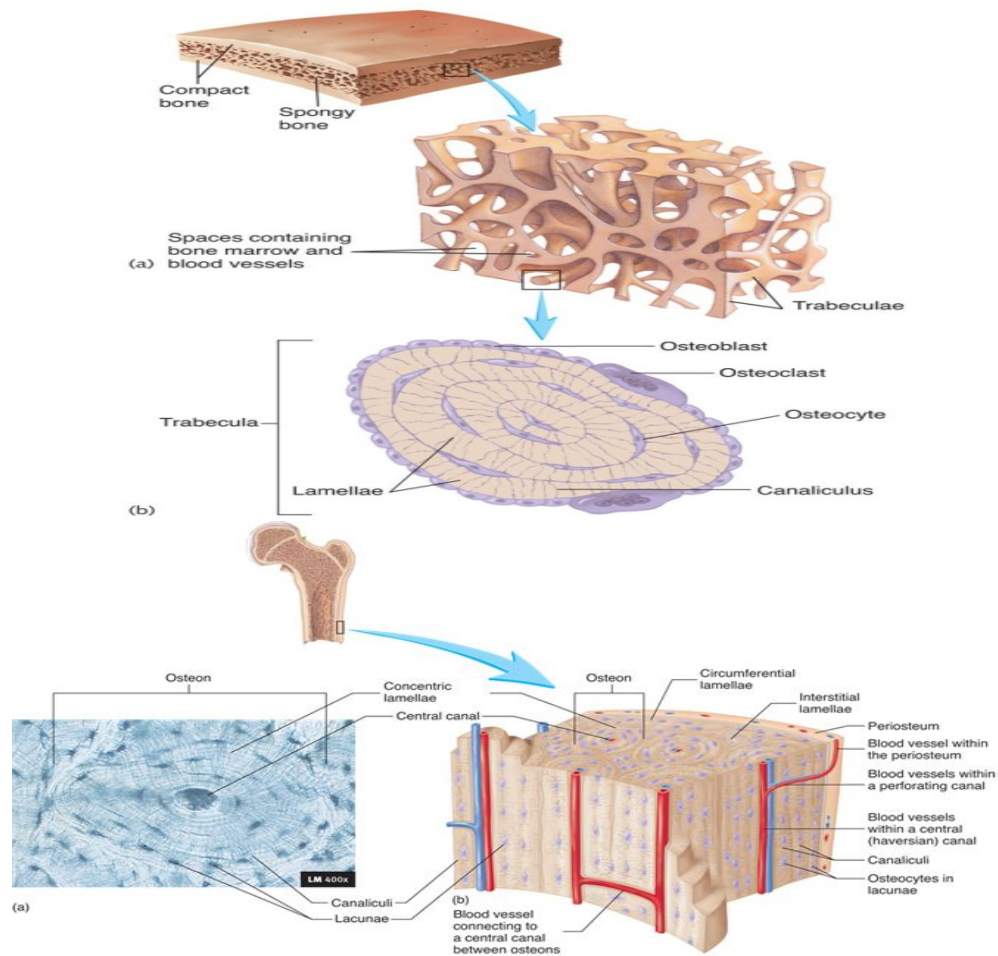
Figure 1. Human Bone Structure

Many bones contain cavities, also called lacuna, filled with marrow. Bone marrow has two different types: red and yellow. Red marrow is the site of blood production while yellow marrow stores adipose tissue. It is only the red marrow which produces red and white blood cells. When the red marrow is surrounded by a framework of reticular fibers it is called hematopoietic. In addition, hematopoietic stem cells reside in the medulla of the bone and have unique ability form different types of blood cells.[21]

### 1.3.2 Bone Histology

The constituents of the bone are bone matrix and bone cells. The major content of the bone matrix is inorganic material and the rest is organic material. The composition of the bone matrix gives the characteristics of bone. The primary constituents of organic material are collagen and proteoglycans while the primary constituent of inorganic material is hydroxyapatite, $[Ca_{10}(PO_4)_6(OH)_2]$.[22] The major functional characteristics of bone are due to collagen and mineral components. The bone matrix is similar to the structure of concrete; collagen fibers give flexible strength to the matrix while weight bearing strength is given by mineral components. [23]

Bone cells can be categorized into three different types: osteoblasts, osteocytes, and osteoclasts. Each type of cells has different functions and they originate from different places. Osteoblasts are bone forming cells which becomes an osteocyte when it is surrounded by bone matrix. The bodies or osteocyte occupies spaces called lacunae and the space osteocyte cell processes are called canaliculi. Osteoclast reabsorbs or breakdowns bone and they also release enzymes that digest protein components of the matrix. Osteochondral progenitor cells become osteoblasts which will become osteocytes. However, osteoclasts are derived from stem cells in red bone marrow. The formation of bone, called ossification or osteogenesis, occurs by appositional growth.[20]

Bone tissue can be categorized into two different types according to the organization of collagen fibers within the bone matrix. While randomly oriented

collagen fibers in many directions it is called woven bone, lamellar bone is when mature bone is organized into thin sheets or layers of lamellae.[20]

According to the amount of bone matrix relative to the amount of space within the bone, both bone tissue types can be differentiated into two different bone types, spongy and compact, as shown in Figure 2. There are more spaces in spongy bone because it is porous because it lacks bone matrix. The interconnecting rods or plates of bone are called trabeculae. The space is filled with bone marrow. However, compact bone has more bone matrix so less space.[20]
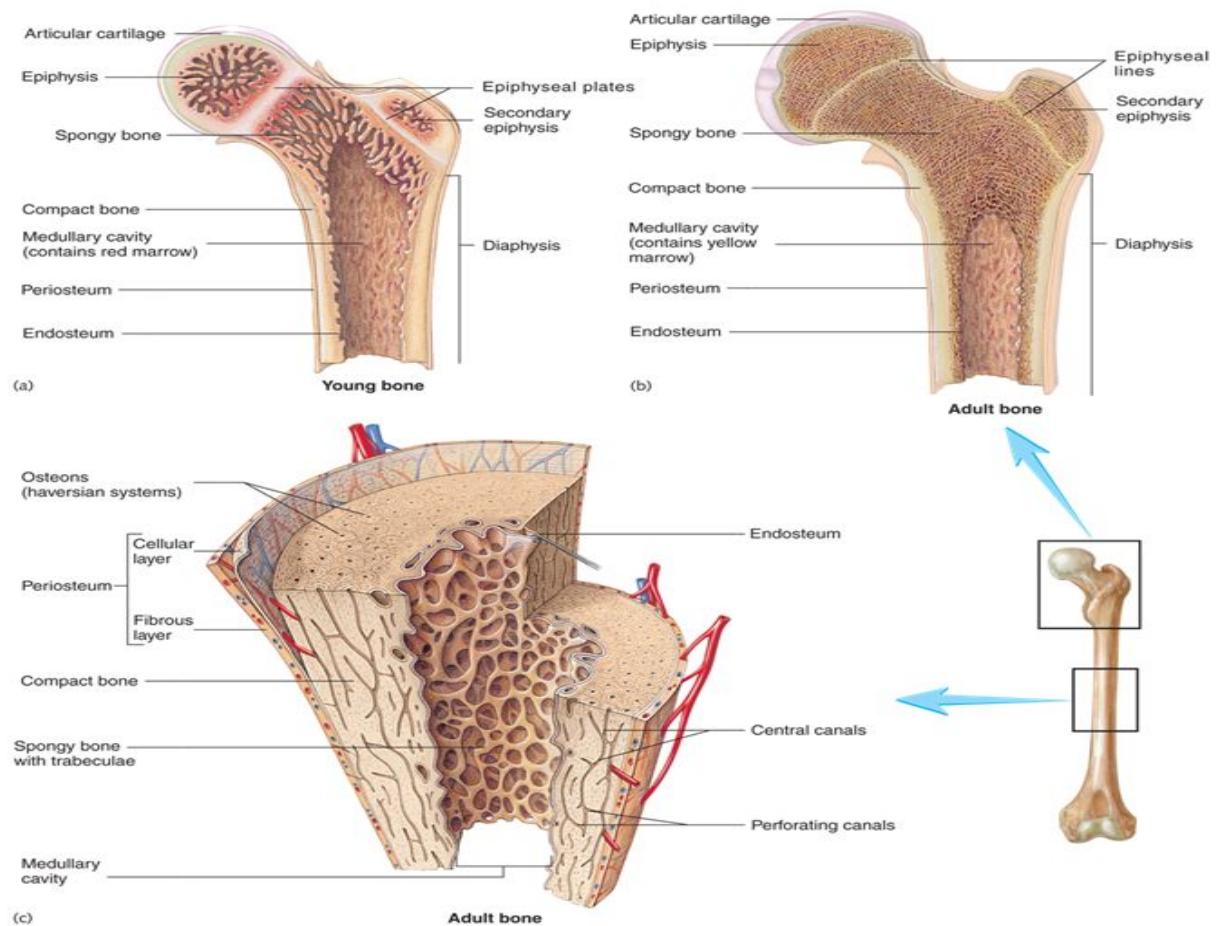


Figure 2. Types of bone

### 1.3.3 Bone Repair

Bone is a living tissue that can undergo repair if it is damaged and the repair process consists of four major steps as shown in Figure 3.[20]

1. Hematoma formation: Bone fracture leads to damages to blood vessels in the bone and surrounding periosteum. Therefore, a hematoma forms which is a localised mass of blood released from blood vessels but confined within an organ or a space. Usually, blood forms clot in hematoma and consisting of fibrous proteins that stop the bleeding.

2. Callus formation: A callus is a mass of tissue that forms at a fracture site and connects the broken ends of the bone. An internal callus forms between the ends of the broken bones, as well as in the marrow cavity if the fracture occurs in the diaphysis of a long bone.

3. Callus ossification: Woven spongy bone replaces the internal and external calluses

4. Bone remodelling: Compact bone replaces woven bone, and part of the internal callus is removed, restoring the medullary cavity.
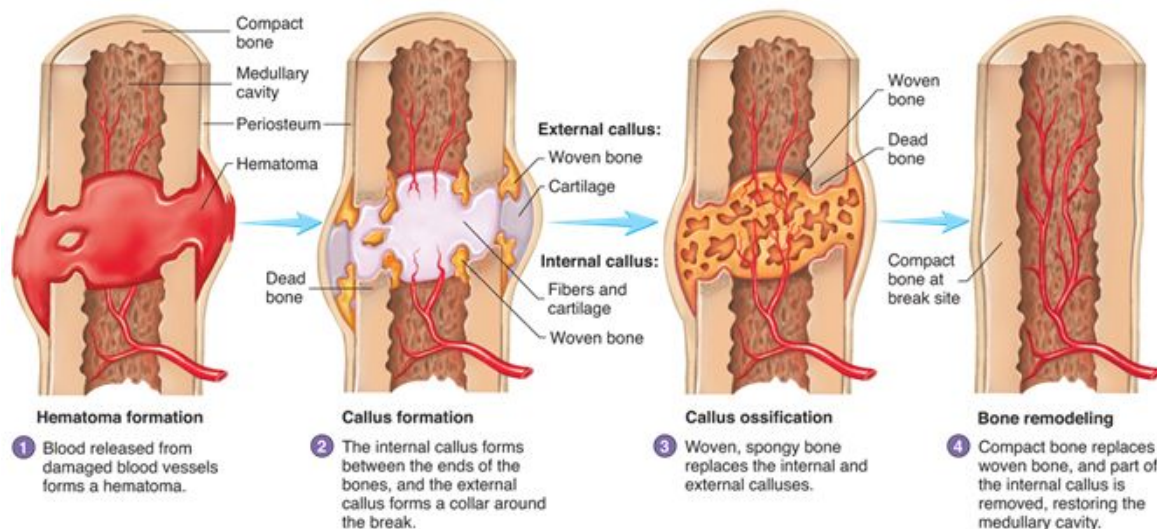
Figure 3. Bone Repair

### 1.3.4 Hydroxyapatite [$Ca_{10}(PO_4)_6(OH)_2$]

Hydroxyapatite is the primary inorganic crystalline constituent of the bone, enamel, dentine and cement. It is also bioactive so it supports the growth of bone by integrating in the newly formed bone tissue without dissolving or breaking down. Carbonate, fluoride, and chloride may replace the hydroxide group which results in thermally less stable apatites. In addition, the substituted apatite has lower mechanical strength. The expected applications of hydroxyapatite as biocompatible phase reinforcement in biomedical composites are:

   a. Coating on metal implantations by altering the surface properties.

   b. Bone fillers; provides a scaffold and encourages the rapid filling of the void by naturally forming bone which provides an alternative to bone grafts and eventually reduces the healing time. [24]

Some published well known methods of producing hydroxyapatite coatings are sol-gel processing, co-precipitation, emulsion techniques, batch hydrothermal processes, mechanical-chemical methods and chemical vapour deposition.[25] However, these methods have critical disadvantages such as high cost of materials needed, precise control over reaction conditions, the use of organic solvents, and time consuming preparation processes. In addition, these methods do not provide sufficient control over particle size, agglomeration surface area, and shape.[26] Furthermore, hydroxyapatite crystallizes out of aqueous solution when the degree of supersaturation is low.

Enormous work has been conducted to develop calcium phosphate bone cement for example to treat hair line fractures but the cement often requires a long time to harden.[27] Incorporation of polymers into the cement paste has been shown to improve this problem, resulting in cement with improved compressive strength and reduced crystalline dimensions.[28]

## 1.3.5 Metal Organic Frameworks (MOFs)

Applications of MOFs include gas storage, gas separation, as well as catalysts but they are almost extensively limited to transition metals. In contrast, the analogous chemistry involving the *s*-block remains at its infancy.[29]

Metal organic frameworks are crystalline compounds consisting of metal ions or clusters coordinated to often rigid organic molecules to form 1-, 2-, or 3-dimensional structures which maybe porous. The organic molecule is often called

a linker and may involve a mono-, di-, tri-, or tetravalent ligand. The type of metal and linker significantly influences the structure and properties of the resulting MOFs. For instance, the metal's coordination ability influences the size and shape of pores by allowing a different number of ligands to bind in different orientations.[30]

The extensive work on MOFs involving phosphorus based ligands in conjunction with transition metals has demonstrated significant array of structural features attainable by judicious ligand and donor choice in phosphonic acid system. The phosphate $[P=O(OH)_2]$ moiety is connected to carbon center either leading to a phosphonate $[RP=O(OH)_2]$ or a diphosphonate $\{R[P=O(OH)_2]\}$ if the carbon backbone connects to two phosphonate moieties. Phosphonic acids can be deprotonated once or twice depending on the conditions; the second deprotonation requiring a stronger basic agent. In contrast, phosphinic acids have only one acidic proton.

Often water is either as coordinative or as water of crystallization in the channels is present if the crystal structure of MOFs is prepared under hydrothermal conditions. The water may be lost in two different ways; typically water in the canals and cavities is lost more easily than coordinated water. However, water lost from cavities may be removed reversibly with the framework intact, but loss of metal coordinated water often leads to structural breakdown and loss of crystallinity.[31] For instance, aluminium diphosphonate $Al_2O_3P(CH_2)_2PO_3H_2O_2F_2 \cdot H_2O$ contains water in the channels but can be removed

between 100 °C and 380 °C. In contrast, the isostructural gallium compound $Ga_2(O_3PCH_2)_2HeO_2F_2.H_2O$ maintains crystallinity upon loss of water. The significant difference in the reversible water loss properties of aluminium and gallium demonstrate how difficult it is to predict these properties and to eventually design a compound to be synthesized. A possible explanation for the reversible water loss might be the larger pore size of gallium species as compared to the aluminium compound.[32] Often other molecules than water can be introduced into the channels, hence the ability of certain MOFs for gas storage.

Furthermore, the reversible loss of water may lead to structural changes with retention of the framework. This is observed in vanadium ethylenediphosphonate complexes.[32] Upon water loss, the complex changes from a square pyramid to a tetrahedral metal environment, resulting in a unique application as absorbent and catalyst. Moreover, it has been shown that fluoride ($F^-$) incorporation improves the formation of crystalline lattices. $F^-$ may introduced by use of HF solutions.

The significant difference in the properties of each framework demonstrates how difficult it is to predict and eventually design a material with desired properties. The most significant characteristics that most researchers focus on is the size of pores.

In biology, the growth of new cells can be enhanced with a scaffold and the general characteristic of scaffold is having pores and an extensive surface

area.[34] Thus, biomimetric and biocompatible MOFs with open pores are being explored in this work to explore their possible use as scaffold for bones in growth.

**1.3.6 Ethylenediphosphonate in metal organic frameworks**

Transition metal based ethylenediphosphonate MOFs are extensively studied, revealing a variety of metal binding modes and deprotonation types of this ligand system. For instance, a double deprotonation is observed in $Sn(HO_3PCH_2PO_3H)$.[25] Whereas quadruple deprotonation is seen in $Ti(O_3P(CH_2)_2PO_3)$ or $Ag_4(O_3P(CH_2)_2PO_3)$.[25,33] Selected MOFs involving diphosphonates and alkaline earth metals have been reported for example a doubly deprotonated ligand is observed in $Ba(HO_3PCH_2CH_2PO_3H)$.[7] Alternatively, but less common single/double diphosphonate deprotonation has been observed in selected examples include $M^{III}(H_2O)(HO_3P(CH_2)_2PO_3)$ where M = Fe, Ga, Al. Alkali metal diphosphonates typically contain a singly deprotonated ligand as seen in $Na(HO_3PCH_2CH_2PO_3H_2)$.[33] The stepwise deprotonation of ethylene diphosphonate and its pH dependence is shown in Figure 5.[35]
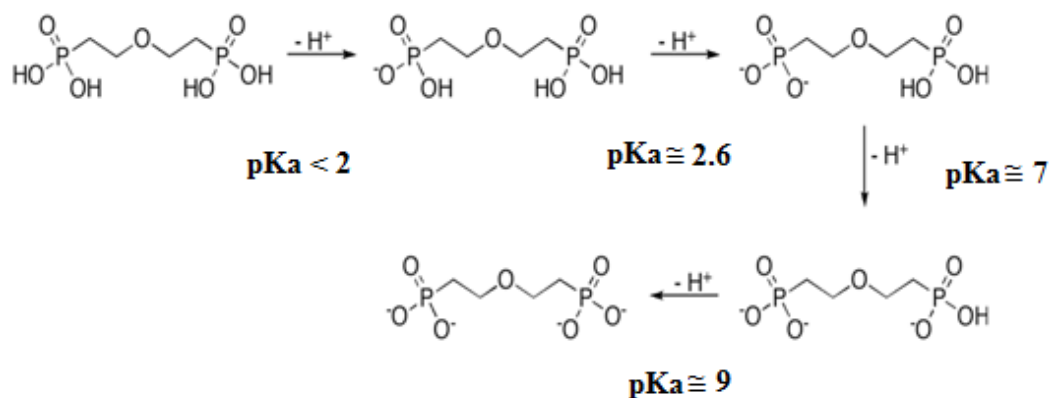
Figure 5. Deprotonation of Ethylene Diphosphonate

While a large number of transition metal diphosphonates are known, only few alkaline earth metal based examples have disseminated.[7, 38-40]

The degree of deprotonation is not always easy to identify, relying on x-ray data and corresponding P-O bond length. P=O bond are typically the shortest, P-O⁻ (1.566 Å) adopt an intermediate bond length while P-OH bonds (1.524 Å) are the longest.[4] A different technique to identify the degree of protonation is based on $^{31}$P MASS NMR spectroscopy. It is very difficult to locate the deprotonation site but Clearfield *et al*. found out the site with $^{31}$P MASS NMR spectroscopy. Their assumptions were later confirmed by studies on isostructural Pr and Gd complexes.[41] As an example, in $Fe(H_2O(HO_3P(CH_2)_2PO_3)$, the protonated, P-OH, has a P-O distance of 1.573 Å being longer than the P-O distances of the deprotonated, P-O⁻ form, 1.503 Å.[36]

In 2007, Tuikka *et al*. reported a series of new barium diphosphonates based on ligand different linker lengths. and obtained single crystals by gel

crystallisation. They observed a correlation between the length of the carbon chain and separation between the layers. Another significant characteristic was that the deprotonation sites were not consistent.

**Chapter 2: Synthesis of diphosphonate ligand and calcium and magnesium based diphosphonates**

**2.1 Synthesis of diphosphonate ligand**

Phosphonate and diphosphonate ligands are often prepared by the Michaelis-Arbuzov reaction as shown in Figure 4 and it involves the treatment of trialkyl phosphite and an alkyl halide to form the phosphonate. This reaction is widely used for the synthesis of various phosphonates, phosphinates and phosphine oxides. The reaction was discovered by Michaelis in 1898 and improved by Aleksandr Arbuzov. [41]
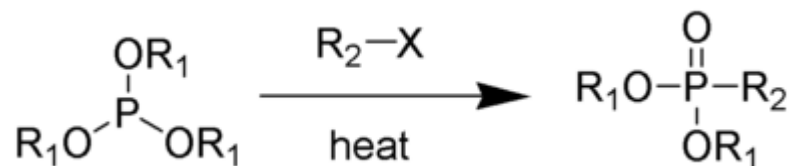
Figure 4. Michaelis-Arbuzov reaction

Phosphorus in the resulting compounds may be in various oxidation states according to which bond is formed, +1, +3, and +5. Examples are shown in Table 2 below.[42]

Table 2. Examples of phosphorus oxyacids

| Name | Oxidation state of P | Structure |
|---|---|---|
| Phosphinic acid $H_3PO_2$ | +1 |  |
| Phosphorous acid $H_3PO_3$ | +3 |  |
| Orthophosphoric acid $H_3PO_4$ | +5 |  |

Simple bisphosphonate esters are often synthesised using Michaelis-Becker syntheses. However, as aforementioned, this project will seek a different synthetic route to obtain high yield products and this is Michaelis-Arbuzov reaction.

The Michaelis-Arbuzov reaction follows a $S_N2$ mechanism involving the reaction of the nucleophilic phosphite (1) with the electrophilic alkyl halide (2) to afford the phosphonium intermediate (3) shown in Figure 6. Triaryl phosphites, which are unable to perform the second step of the Michaelis-Arbuzov reaction, have been shown to produce stable phosphonium salts. Likewise, aryl and vinyl halides are less reactive towards phosphites. The displaced halide anion reacts via

another $S_N2$ reaction with the phosphonium intermediate to give the desired phosphonate (4) and another alkyl halide (5).[30]
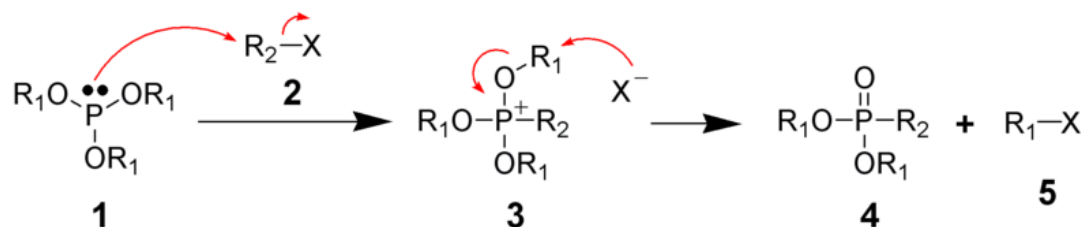
Figure 6. Stepwise mechanism of Michelis-Arbuzov Reaction

The choice of ligand, 3-oxapentane-1,5-diphosphonic acid, is based on the special properties and binding modes it may have compared to previously used ligands such as ethylene diphosphonic acid and butylenes diphosphonic acid. Hence, I expect to see different products that will exhibit different coordination and aggregation characteristics. Due to the geometric shape and length of 3-oxapentane-1,5-diphosphonic acid we expect the formation of materials with open and connecting channels which may be crucial for a scaffold bone material. Previous studies done by other students in the lab have shown that different backbone chains have an effect on the binding mode and metal coordination.

## 2.2 Synthesis of calcium and magnesium diphosphonate compounds

The main focus of this study was on alkaline earth metal especially calcium and magnesium due to their presence in most biological systems. Variables utilized in the synthesis of the Mg and Ca based target compounds include pH, introduction of various lewis bases, as well as different temperatures.

The pH of some reactions was adjusted to pH 7 using sodium hydroxide because the ligand is acidic (pH 1). The reactions were conducted in water as well as methanol and ethanol. The temperature range applied varied from room temperature to 150°C. Lewis bases used include 1,4-diazabicyclo[2.2.2]octane (DABCO), tetrahydrofuran (THF) and dimethylformamide (DMF). Among many reactions only three reactions yielded precipitate. These are all listed in detail below. All reactions were run with hydrothermal reaction.

Hydrothermal synthesis is based on the increased solubility of reagents and products under high pressure and high temperature conditions. The improved solubility will facilitate crystal growth. Hydrothermal conditions applied in this work. The reaction is conducted in a thick walled glass sealed under reduced pressure at temperatures above the boiling point of the solvent in this case, water. As the water evaporates the, pressure increases. The method has been advantageous for the growth of good quality crystals. When the solvent is not water, the process is called solvothermal.[40] All product yielded reactions were maintained the temperature of 150 °C at a pressure not exceeding 15 atm.

**Chapter 3: Results and Discussion**
**3.1 Results**

**3.1.1 Preparation of Ligand, 3-Oxapentane-1,5-bisphosphonic Acid**
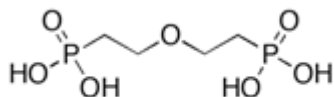


3-oxapentane-1,5-bisphosphonic acid

The ligand, 3-oxapentane-1,5-bisphosphonic acid, was prepared utilizing well known reaction Michaelis-Arbuzov. 2-bisbromoethyl ether was added to excess triethyl phosphite. One of the reaction product, ethyl bromide, and excess triethyl phosphite was removed from the reaction by distillation. As a result, the reaction was straightforward as only the two reactants are present, still, by-products and excess reactants required removal. The ratio of the 2-bisbromoethyl ether : triethyl phosphite reagent was used in a (1:7 ratio) to speed up the reaction and ensure the completion of the reaction.

The critical step in the reaction to improve yield is to remove the volatile by-products, ethyl bromide, but also the excess reagent, triethyl phosphite. This can be achieved by distillation. In addition, the key feature of this reaction was to keep the reaction temperature below the boiling point of 2-bisbromoethyl ether to improve the yield. The reason was that 2-bisbromoethyl ether was the limiting agent and has a lower boiling point than triethyl phosphite. Furthermore, once the reaction ceased the reaction mixture was left under vacuum over night to remove undesired relative chemicals left and produced in the reaction.
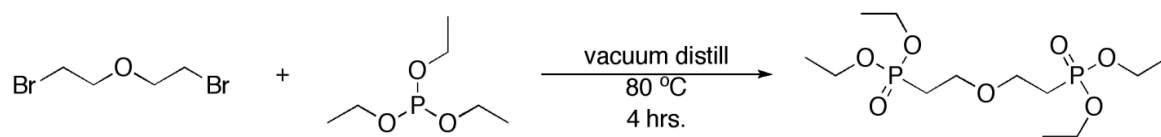
Figure 7. The first step of synthesis

The product formation was confirmed by the $^1$H NMR spectroscopy and the target ester was also confirmed by $^1$H NMR spectroscopy, a spectrum is shown in Figure 7.
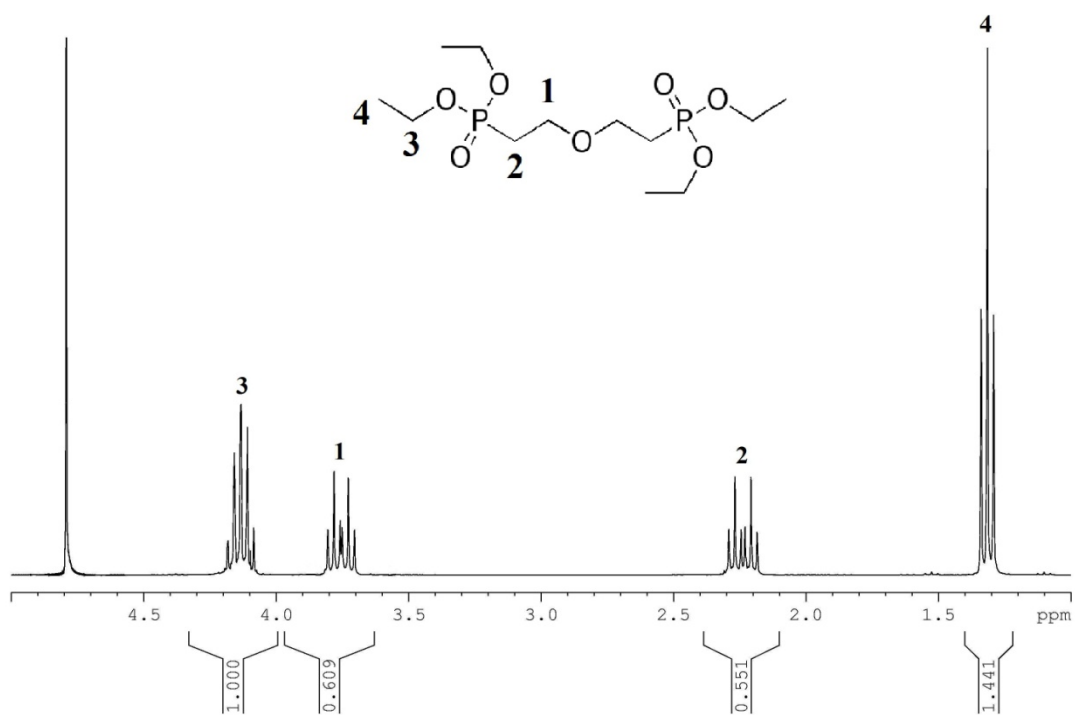


Figure 7, NMR of intermediate product ester, $C_{12}H_{28}O_7P_2$

A further reaction step is necessary to transform the ester into the desired acid. This can be achieved by treatment with concentrated hydrochloric acid followed by reflux for 3 days. Excess acid was added to ensure complete the hydrolysis of the ester. After three days, the reaction mixture was concentrated under reduced pressure. The methanol was used to remove the ethyl chloride, by-product. This was only possible since ethyl chloride and methanol are azeotropes. Azeotropes are a mixture of at least two different liquids. Their mixture can either have a higher boiling point than either of the components or they can have a lower boiling point.[40] Azeotropes occur when fraction of the liquids can't be altered by distillation. The azeotropic mixture of compounds in this case includes ethyl chloride and methanol. Moreover, the product was also treated with diethyl ether to dry further**.**
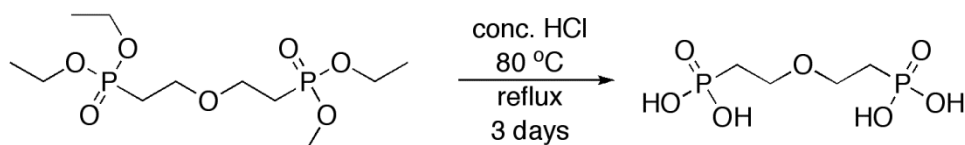


Figure 8. Second step of synthesis

Lastly, the ligand was treated with acetonitrile for further purification and the results are shown in Figure 9 and 10. The circled peaks disappeared after the product was treated with acetonitrile. The peaks are due to impurities because the peaks are not starting materials and also the yellow color was gone to yield white product.
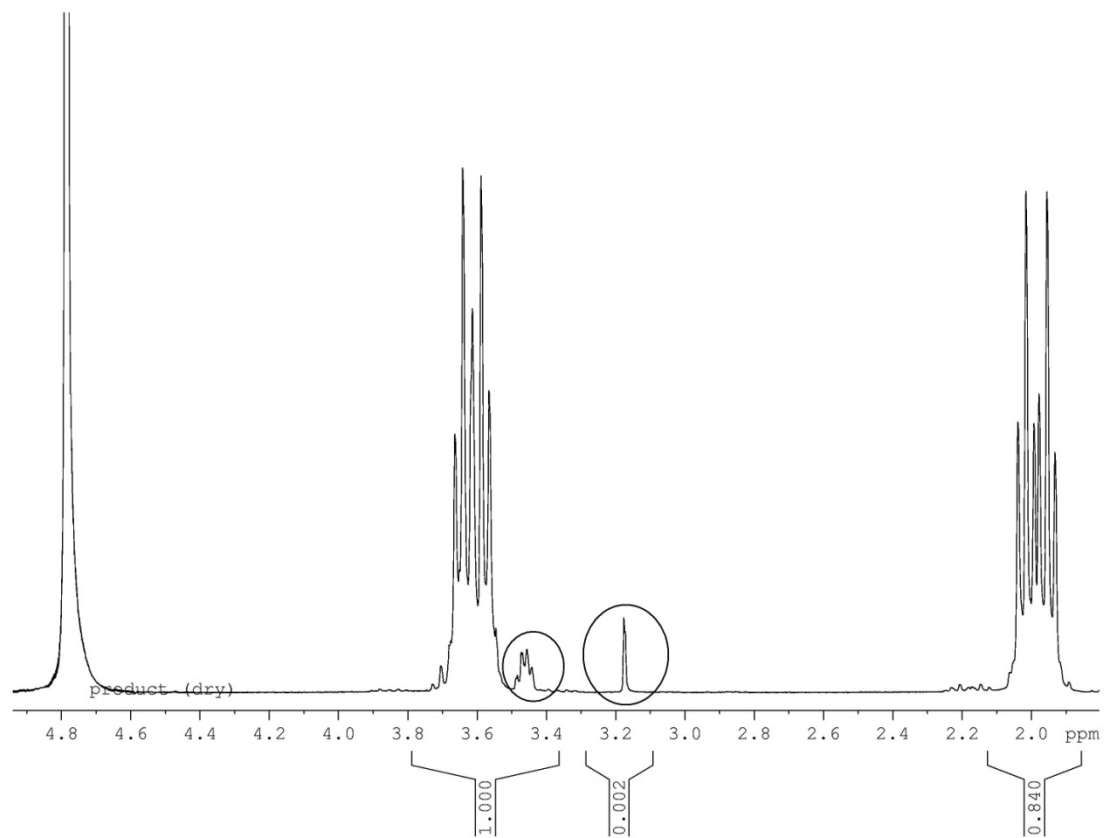
Figure 9, NMR of ligand before treated with acetonitrile
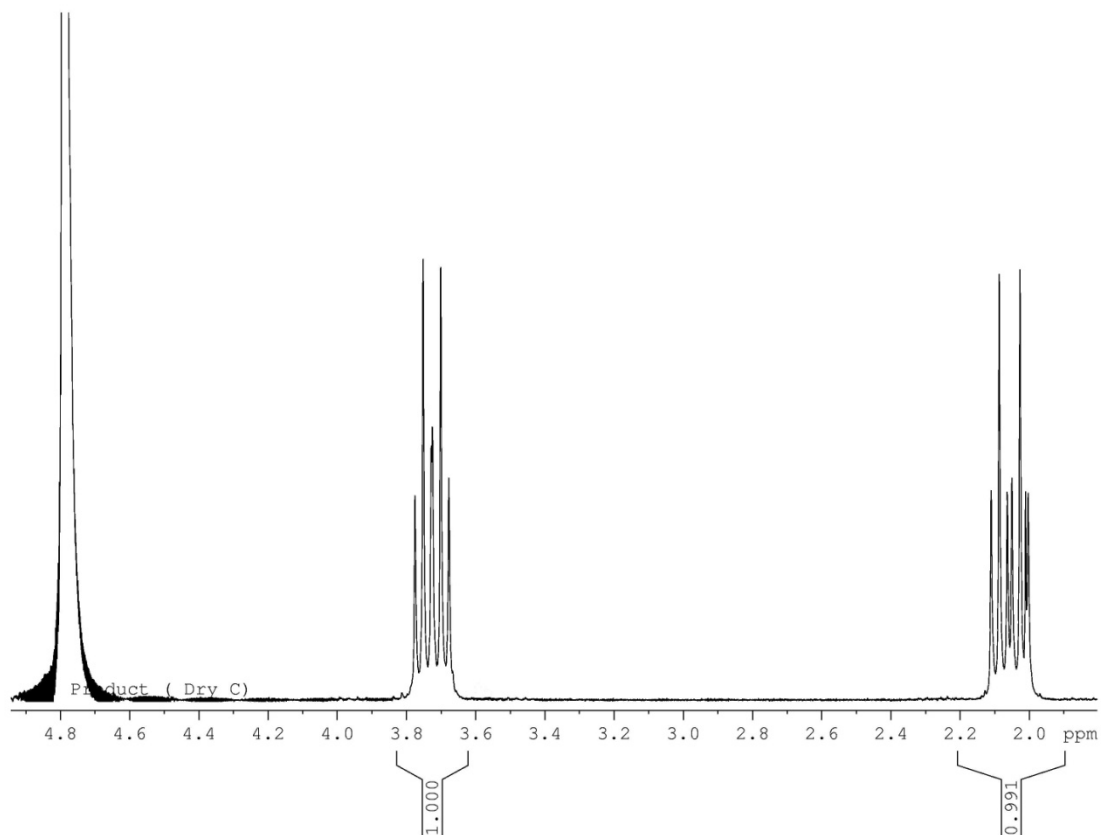
Figure 10, NMR of ligand after treated with acetonitrile

The analytical methods including melting point, ^{1}H-NMR, and IR spectroscopy were done beside single X-ray crystallography.

The physical and chemical properties of the ligand were explored such as solubility of ligand, pH, and melting points. These physical and chemical properties were considered in designing the reactions.

### 3.1.2 Synthesis of calcium diphosphonate



Product 1 was obtained hydrothermally from the reaction of ligand and calcium chloride (anhydrous) in the ratio of 1:1 using water as solvent. The reaction was prepared in a Carius tube and the reaction mixture was pH 1. Once the tube was sealed under reduced pressure it wa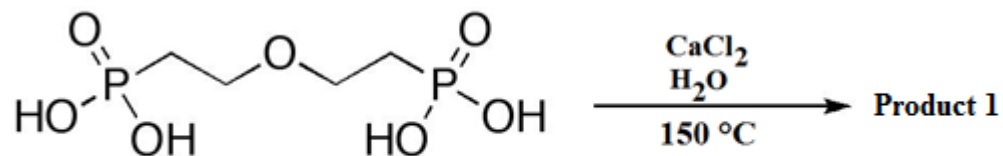s placed in 150°C oven. When it was placed in the oven the volume of solution reduced but once it was taken out the volume increased to its starting volume. The reaction mixture remained clear after a week in the oven. Thus, the volume of the reaction mixture was reduced by heating with heat mantle and left at room temperature for crystallization. It took about a month for precipitation to occur. Attempts to characterize the product by single X-ray crystallography failed due to poor crystal quality. Three alternative methods, melting point, IR and $^1$H NMR, were carried out in order to analyze the product. These methodologies suggest product formation, but do not allow the prediction of the exact product composition.

Comparison of the product's melting point with $CaCl_2$ and ligand shown in Table 3 indicate that the melting point is significantly higher than the free ligand, with a decomposition temperature of 262 °C. Previous students who worked with similar compounds have suggested that the high melting point of

compound provides evidence that product formation took place. ^{1}H NMR spectroscopic analysis in $D_2O$ shows a slight shift in chemical shift between the ligand and the reaction product, providing some indication that the ligand is apparent in a deprotonated form. Figure 11 shows the comparison of the ligand and the reaction product.

Table 3. Melting point comparison for compound 1

|  | Meting point (°C) |
| --- | --- |
| Ligand | 119-121 |
| CaCl$_2$ | 775 (anhydrous)<br>45.5 (tetrahydrate)<br>175 (dihydrate)<br>30 (hexahydrate) |
| Compound 1 | 262 (decomposition) |

Figure 11. ^{1}H NMR spectra for comparison of chemical shifts of the free ligand
and compound 1

The ^{1}H NMR spectrum which may suggest product formation due to small
changes of the chemical shifts, as summarised in Table 4. The metal coordination
influences the protons in compound when they interact with a part of a compound
which leads to the changes in the chemical shift observed in the ^{1}H NMR.[38]

Table 4. Chemical shift comparison for ligand and product 1

|  | Ligand | Product 1 |
|---|---|---|
| Chemical shift (ppm) | 2.06, 3.73 | 2.04, 3.75 |

### 3.1.3 Synthesis of magnesium diphosphonate
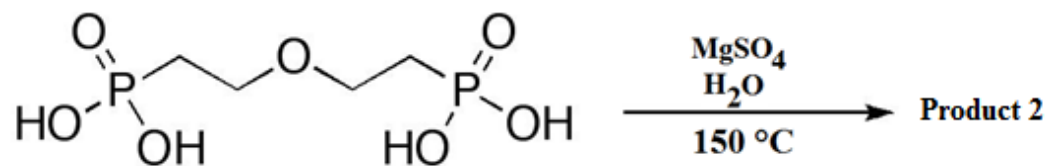


Product 2 was obtained hydrothermally from the reaction of ligand and magnesium sulphate (anhydrous) in the ratio of 1:1 using water as solvent. The reaction mixture was prepared in a Carius tube and it was placed in 150°C oven once sealed under reduced pressure. The reaction mixture was milky but became clear after a week in the oven. To induce crystallisation the volume of the solvent was reduced by heating with heat mantle and left at room temperature. However, crystal quality prevented characterization by single X-ray crystallography. Three alternative methods, melting point, IR and $^1$H NMR, were carried out in order to analyze the product. These methodologies suggest product formation, but do not allow the prediction of the exact product composition. See Table 5.

Table 5. Melting point comparison for compound 2

|  | Meting point (°C) |
|---|---|
| Ligand | 119-121 |
| MgSO$_4$ | 200 (monohydrate) 150 (heptahydrate) |
| Compound 2 | 272 (decomposition) |

As it is shown in Table 5, the melting point of the product is not close to neither the ligand nor the magnesium sulphate but with a melting point of 272 °C. The temperature is quite similar to compound 1.
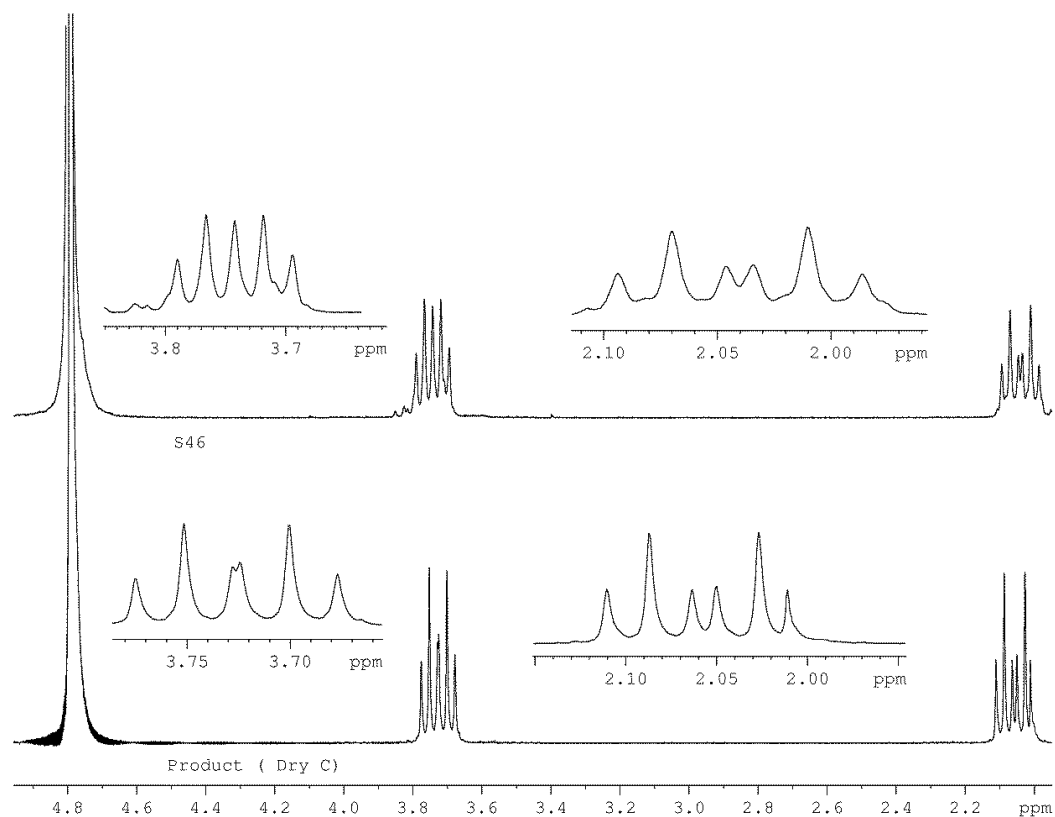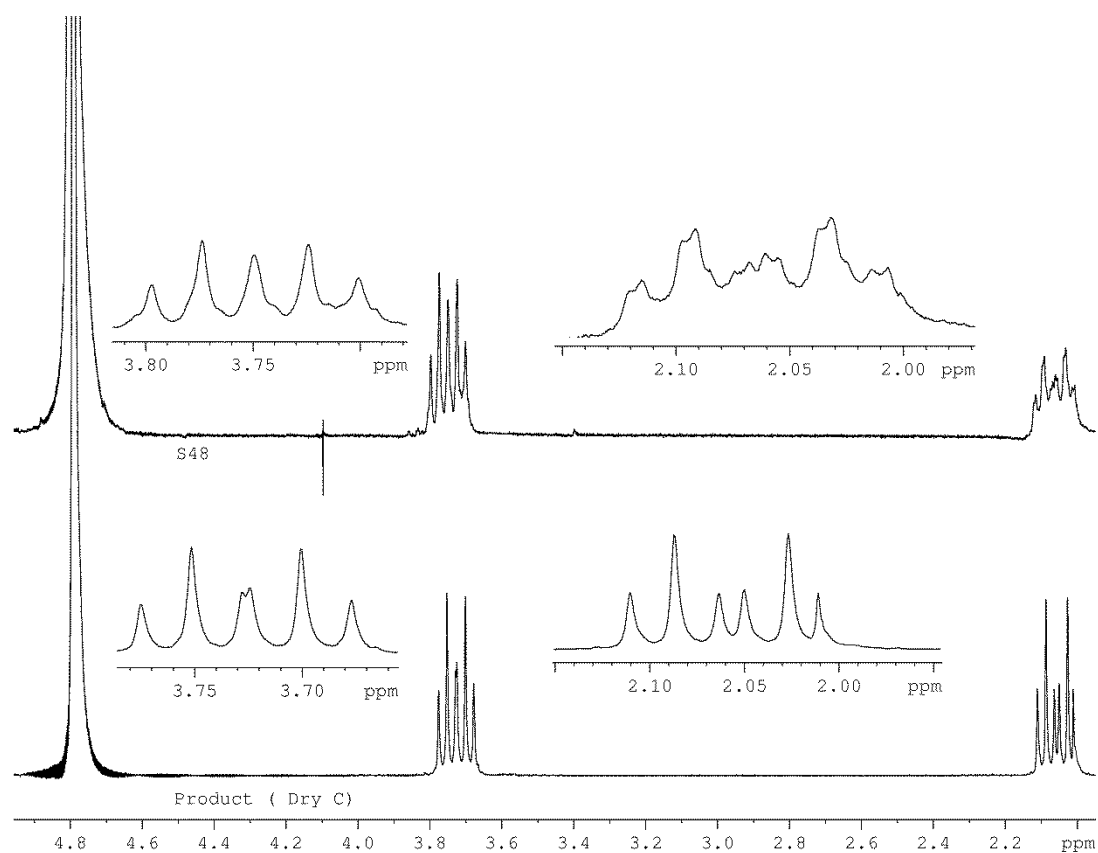


Figure 12. ^{1}H NMR spectra comparison of chemical shifts for free ligand and compound 2

The ^{1}H NMR spectrum which may suggest product formation due to small changes of the chemical shifts, as summarized in Table 6. The metal coordination

influences the protons in compound when they interact with a part of a compound which leads to the changes in the chemical shift observed in the $^1$H NMR.[38]

The $^1$H NMR shows similar characteristic changes observed in compound 1. The chemical shifts became slight downfield compared to the ligand. Table 6 provides chemical shifts of free ligand and compound 2 for comparisons.

Table 6. Chemical shift comparison for ligand and product 2

|  | Ligand | Compound 2 |
| --- | --- | --- |
| Chemical shift (ppm) | 2.06, 3.73 | 2.06, 3.75 |

### 3.1.4 Synthesis of calcium diphosphonate
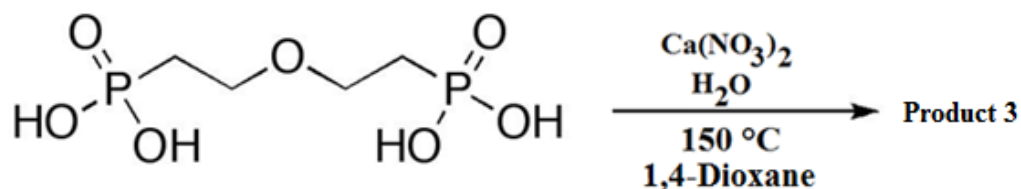


Compound 3 was obtained hydrothermally from the reaction of the ligand and calcium nitrate in the ratio of 1:1 with water as solvent. The reaction mixture was prepared in a Carius tube and placed in 150°C once it was sealed under reduced pressure. The reaction mixture was still clear after a week in the oven. Thus, the volume of the reaction mixture was reduced by heating with heat mantle and left at room temperature for crystallization. It took a month to observe the

formation of precipitate. However the crystallinity of the solid did not allow it's characterization by single X-ray crystallography.

As shown in Table 7, the melting point of the product does not compare to ligand or the calcium nitrate starting material. The product actually decomposed at 270 °C.

$^1$H NMR spectroscopy in $D_2O$ indicated a slight change in chemical shift for the reaction product, similar to those observed for compounds 1 and 2

Table 7. Melting point comparison for compound 3

|  | Meting point (°C) |
|---|---|
| Ligand | 119-121 |
| $Ca(NO_3)_2$ | 42.7 (tetrahydrate) |
| Compound 3 | 270 (decomposition) |

Table 8 provides chemical shifts of free ligand and compound 3 for a comparison.

Table 8. Chemical shift comparison for ligand and product 3

|  | Ligand | Compound 3 |
|---|---|---|
| Chemical shift (ppm) | 2.06, 3.73 | 1.99, 3.73 |
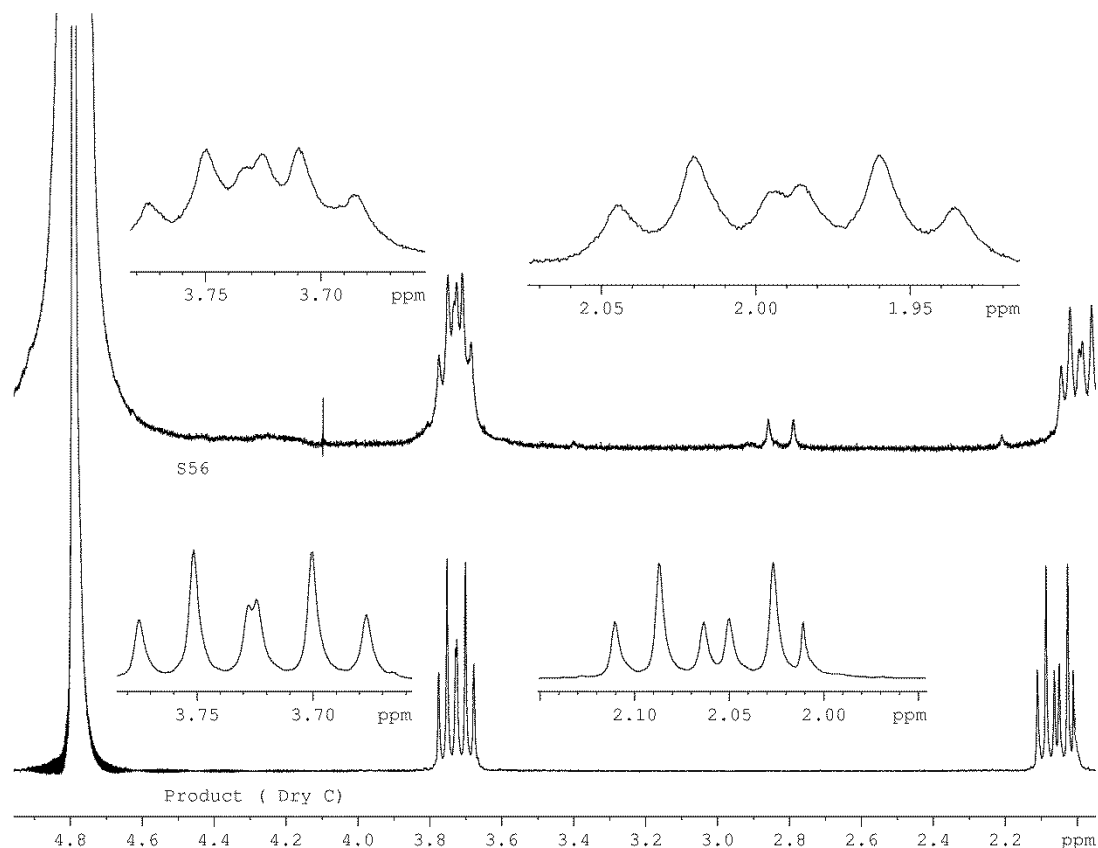
Figure 13. ^{1}H NMR spectra comparisons of chemical shifts of the free ligand and compound 3

In summary, the data obtained from analysis provide the motivation for further studies, specifically with the aim to produce high quality crystals that can be analyzed with single X-ray crystallography. Table 9 provides the analytical values obtained from characterizations- clearly slight changes in chemical shifts are observed and distinct peaks in finger print region in IR spectrum are observed for each compound.

Table 9. Values for $^1$H NMR and IR spectroscopy

|  | Ligand | Compound 1 | Compound 2 | Compound 3 |
|---|---|---|---|---|
| Chemical shifts (ppm) | 2.06, 3.73 | 2.04, 3.75 | 2.06, 3.75 | 1.99, 3.73 |
| Chemical shift change (ppm) | N/A | -0.02, +0.02 | 0, +0.02 | -0.07, 0 |
| IR spectroscopy peaks | 2920(w), 2723(s), 1468(s), 1389(s), 1303(s), 1154 (s) 1037(s), 933(s), 722(s) | 2920(s), 2853(s), 1458(s), 1376(s), 1154(s), 1053(s), 928(s), 846(s), 722(s), | 2919(w), 2723(s), 1465(s), 1374(s), 1154(s), 1065(s), 933(s), 846(s), 722(s) | 2920(s), 2850(s), 1458(s), 1376(s), 1154(s), 1042(s), 912(s), 845(s), 722(s); |

## 3.2 Discussion

Transition metal phosphonates are well represented in the literature. In contrast, significantly less is known about the very challenging *s*-block metal.

A range of significant differences between the two groups of metals is apparent, including the larger size of the *s*-block metals. The large size of the *s*-block metals results in large coordination numbers and a pronounced tendency towards aggregation. The absence of energetically available d-orbital for the *s*-block metals, along with the electropositive characters for the *s*-block metals result in mainly electrostatic bonds and s-orbital control.

The primary goal of this project was to develop synthetic routes to design and synthesize magnesium and calcium phosphonates to develop methodologies to obtain high quality crystals of the products. During the project a number of synthetic methods and reaction conditions were employed. Furthermore, attempts were made to improve the crystallinity of the reaction products. Technique employed included the addition of co-ligands (lewis bases) but no improvement was noticed.

**Chapter 4: Experimental**

**4.1 General Methods:**

**Reactions:** All reactions were performed in hydrothermal condition except for the synthesis of the ligand. A wide range of temperature of the oven was used beginning from low temperature to high temperature. Reaction solvents were selected according to the solubility of the ligand.

**Analysis:** $^1$H-NMR spectra were recorded on Bruker Avance 300 spectrometer at 300 MHz using $D_2O$ and $CDCl_3$. The chemical shifts are given in parts per million (ppm). Coupling constants are reported in Hertz (Hz). The solvent peak was used as a reference value, for $^1$H-NMR: $CDCl_3$ = 7.27 $D_2O$ = 4.8. Data are reported as follows: (s = single; d = doublet; t = triplet; q = quartet; p = pentet; dd =doublet; dt = doublet of triplets; td = triplet of doublets; bs = broad singlet). IR spectra were obtained with a Thermo Nicolet IR – 100 spectrometer on KBr plates. The melting point was taken with EZ melt – SRS (Stanford Research Systems).

**4.2 Synthesis of Ligand, 3-Oxapentane-1,5-bisphosphonic Acid**

Bis(2-bromoethyl)ether (13.12 g, 8.67 mL, 0.069 mol) and 85.74 mL (0.5 mol) of triethyl phosphite were added to a 250 mL three-neck round-bottom flask. The reaction mixture was then refluxed for 3 hours at approximately 80 °C followed by vacuum distillation at 80 °C until all excess triethyl phosphite was removed. $^1$H-NMR spectroscopy was used to check the completion of the reaction. The ester was treated with 50 mL of concentrated HCl and refluxed for 3

days at approximately 80 °C. The crude bisphosphonic acid was treated with MeOH (5 x 10 mL) and concentrated under reduced pressure, treated with $Et_2O$ (20 mL) and finally concentrated under reduced pressure to yield a clear yellow oil. The crude diphosphonic acid was allowed to dry in room temperature and pressure for a week to obtain product. Solidified diphosphonic acid was washed with acetonitrile to yield white crystalline solid (13.7 g, 85%, mp 119-121 °C;): $\nu$ $_{max}$(KBr)/ $cm^{-1}$ 2920(w), 2723(s), 1468(s), 1389(s), 1303(s), 1154 (P=O), 1037(s), 933(s), 722(s) ; pH 1; $\delta_H$ ($D_2O$) 2.05 (4 H, dt, $^3J_{HH}$ 6.9, $^3J_{HP}$ 18), 3.72 (4 H, dt, $^3J_{HH}$ 6.9, $^3J_{HP}$ 15.3)

### 4.3 Synthesis of calcium diphosphonate

Calcium chloride anhydrous (0.555 g, 5 mmol) and ligand 3-oxapentane-1,5-bisphosphonic acid (1.2 g, 5 mmol) were dissolved in $H_2O$ (4 mL) in a Carius tube. The Carius tube was sealed under reduced pressure and placed in 150 °C oven. The clear solution was taken out of the oven after a week and the volume was reduced and left in room temperature for crystallisation. The solution slowly evaporated to yield a colorless solid after one month; mp 262 °C (decomposition); $\nu_{max}$(KBr)/ $cm^{-1}$ 2920(s), 2853(s), 1458(s), 1376(s), 1154(s), 1053(s), 928(s), 846(s), 722(s), pH 1; $\delta_H$ ($D_2O$) 2.04, 3.75

### 4.4 Ligand and magnesium sulfate in water

Magnesium sulfate anhydrous (0.6 g, 5 mmol) and ligand 3-oxapentane-1,5-bisphosphonic acid (1.2 g, 5 mmol) were dissolved in $H_2O$ (4 mL) in a Carius

tube. The Carius tube was sealed under reduced pressure and placed in 150 °C oven. The clear solution was taken out of the oven after a week and the volume was reduced and left at room temperature for crystallisation. The solution slowly evaporated to yield clear salts after a month in room temperature and pressure; mp 272 °C (decomposition); $\nu_{max}$(KBr)/ cm$^{-1}$ 2919(w), 2723(s), 1465(s), 1374(s), 1154(s), 1065(s), 933(s), 846(s), 722(s); pH 1; $\delta_H$ (D$_2$O) 2.06, 3.75

## 4.5 Synthesis of calcium diphosphonate

Calcium nitrate tetrahydrate (0.236 g, 1 mmol) and ligand 3-oxapentane-1,5-bisphosphonic acid (0.24 g, 1 mmol) were dissolved in H$_2$O (4 mL) in a Carius tube. 1,4-Dioxane (0.176 g, 1 mmol) was added to the reaction mixture. The tube was sealed under reduced pressure and placed in 150 °C for a week. The clear solution was taken out of the oven and the volume was reduced and left in room temperature and for crystallization. The precipitate began to form after 3 weeks later; mp 270 °C (decomposition); $\nu_{max}$(KBr)/ cm$^{-1}$ 2920(s), 2850(s), 1458(s), 1376(s), 1154(s), 1042(s), 912(s), 845(s), 722(s); pH 1; $\delta_H$ (D$_2$O) 1.99, 3.73

**Chapter 5: Conclusions and Recommendations**

In summary, the project entailed the ligand synthesis and once the ligand was obtained the ligand was treated with various magnesium and calcium salts. In three instances calcium chloride in water, magnesium sulphate in water, and calcium nitrate in water in addition to 1,4-dioxane a solid reaction product was obtained. Three products were obtained via hydrothermal synthesis and were analysed using melting point, IR and ^{1}H-NMR. Unfortunately, the detailed analysis could not be obtained because desired single crystals were not obtained.

Three characterizations have shown a possibility of product formation in each reaction. These include slight shifts in the ^{1}H NMR spectra as compared to the starting materials, indicating that some chemical changes must have occurred during the hydrothermal reaction. In addition, the melting point of each product was different from the starting materials. They actually decomposed which provides a strong evidence of product formation.

Future work will include the further exploration of reaction conditions and crystallization methods, including the addition of lewis bases, as well as other magnesium and calcium salts. There are many more changes that can be made in order to obtain high quality crystals.

**WORK CITED**

1. Ray R.; Degge j; Gloyd P; Mooney G, Bone regeneration. *Journal of bone and joint surg. American volume*, **1952**, 34A(3) :638-647

2. Hu, J.; Zhao, J.; Hou, H.; Fan, Y. Syntheses, structures and fluorescence studies of two new cadmium(II) pyridyl-diphosphonates *Inorganic Chemistry Communications* **2008**, 11, 1110-1112.

3. Mao, J. G.; Wang Z.; Clearfield A. Synthesis, Characterization, and Crystal Structures of Two New Divalent Metal Complexes of *N,N'*-Bis(phosphonomethyl)-1,10-diaza-18-crown-6:□ A Hydrogen-Bonded 1D Array and a 3D Network with a Large Channel *Inorg. Chem*. **2002**, 41, 3713-3720

4. Merrill, C. A.; Cheetham, A. K. Inorganic−Organic Framework Structures; M(II) Ethylenediphosphonates (M = Co, Ni, Mn) and a Mn(II) Ethylenediphosphonato-phenanthroline *Inorg. Chem*. **2007**, 46, 278-284

5. Poojary, D. m.; Zhang, B.; Clearfield, A. *J.* Pillared Layered Metal Phosphonates. Syntheses and X-ray Powder Structures of Copper and Zinc Alkylenebis(phosphonates *Am. Chem. Soc.* **1997**, 119, 12550-12559.

6. Ouellette, W.; ming, h. Y.; O'connor, C. J.; Zubieta, Evolution of the Structural Chemistry of Vanadium Organodiphosphonate Networks and Frameworks:□ Structural Consequences of Fluoride Incorporation in the Development of Stable Phases with Void Channels *J. Inorg. Chem*. **2006**, 45, 7628-7641.

7. Tuikka, M.; Haukka, M.; Ahlgren, M. Three barium diphosphonates with 3-D structure *Solid State Sciences* **2007**, 9, 535-541.

8. Harada, S.; Rodon G. A, Mechanism of action of bisphosphonates, *Nature* **2003**, 423, 349-355

9. Jomaa, H; Wiesner J.; Sanderbrand, S.; Altincicek B.; Weidemeyer C; Hintz M.; Turbachova Ieberl M.; Zeidler, Lichtenthaler H. K.; Soldati D.; Beck E. Inhibitors of the nonmevalonate pathway of isoprenoid biosynthesis as antimalarial drugs Sciece, **1999**, 285, 1573-1576

10. Komath, M.; Varma h. K.; Sivakumar R., On the development of an apatitic calcium phosphate bone cement Bulletin of Material Science, **2000**, 23, 2, 135-140.

11. National Aeronautics and Space Administration (NASA), Use of diphosphonates to correct disorders in calcium metabolism and mineral composition of bone tissue with 6-day hypokinesis in rats, **1988**, 205456, Washington

12. Zhang, Y.; Leon A.; Song Y.; Studer D.; Haase C.; Koscielski L.A.; Oldfield E, Activity of Nitrogen-Containing and Non-Nitrogen-Containing

Bisphosphonates on Tumor Cell Lines *Journal of Medicinal Chemistry*, **2006**, 49, 5804-5814

13. Albee, F. H. M.D.; Morrison, H. F. M.D., Studies in Bone Growth: Triple Calcium Phosphate As A Stimulus To Osteogenesis, *Annals of Surgery*, **1920**, 71, 32-39

14. Robert L. R., Jacob J. G., Eva S., Excision of Pseudotumor with Repair by Bone Graft of Pathological Fracture of Femur in Hemophilia, *Journal of Bone and Joint Surgery*, **1973**, 55, 827-832

15. Yardley, V.; Khan A. A.; Martin, M. B.; Shiffer, T. R.; Araujo, F. G.; Moreno S. S.; Docampo R.; Croft S. L.' Oldfield E. A. *Agents Chemother*, **2002**, 46, 929-931

16. Rodgriguez, N.; Bailey B. N.; Martin M. B.; Oldfoeld E.; Urbina, J. A.; Docampo. R. J. *Infective Diseases*, **2002**, 186, 138-140

17. Harada, S.; Rodon G. A. *Mechanism of Action of Bisphosphonates, Nature,* **2003**, 423, 349-355

18. De Graff, V.; Kent, M. *Human Anatomy*, 5th ed., McGraw-Hill, MA., **1998**; 54-60

19. Applegate, E. J. *The Anatomy of Physiology of Learning Systems*, Textbook. W.B. Saunders Company, Philadelphia, 1995

20. Seeley, Rod R. *Seeley's Anatomy & Physiology*. New York, NY: McGraw-Hill, **2011**.

21. Coico, R., and Geoffrey S.. *Immunology: A Short Course*. Hoboken, NJ: Wiley-Blackwell, **2009**.

22. Cukrowski, I.; Popovic, L.; Barnard, W.; Paul, S. O.; van Rooyen, P. H.; Liles, D. C. *Bone*, **2007**, 41, 668-678

23. Fan, E. et al, Body Structure and Function, 7th Ed.; Delmar Publishers Inc. New York, **1989**, 84-86

24. Hench, Larry L. "Bioceramics." *Journal of the American Ceramic Society* 81.7 **1998**: 1705-728. Print

25. Bigi, A.; Boanini, E.; Rubini, K. Hydroxyapatite gels and nanocrystals prepared through a sol-gel process, *Journal of Solid State Chemistry*, **2004**, 177, 3092-3098

26. Aif, A.; Haque S.; Kellici S.; Boldrin P.; Rehman I.; Fazal A. Khalid; Jawaad A. Darr Instant nano-hydroxyapatite: a continuous and rapid hydrothermal synthesis, *Chemistry Communication*, **2006**, 2286

27. Bohner, M. Controlling the reactivity of calcium phosphate cements , *Journal of Materials Chemistry*, **2008**, 18, 5669

28. Mickiewiczm, R. A. *Polymer-Calcium Phosphate Composites for Use as Injectable Bone Substitue*, M.S. Thesis, The Massachusetts Institute of Technology, June **2001**

29. Whang, D.; Hur N. H.; Kim K., A Novel Microporous Mixed-Transition-Metal Phosphate: Hydrothermal Synthesis, Characterization, and Structure of $Zn_2Co_4(PO_4)_4(H_2O)_5.2H_2O$, *Inorganic Chemistry*, **1995**, 34, 3363-3366

30. Czaja, A. U.; Trukhan, N.; Müller, U. (2009). "Industrial applications of metal-organic frameworks". *Chemical Society Reviews* **38** (5): 1284–1293.

31. Devi, R. N., P. Wormald, P. A. Cox, and P. A. Wright. "Novel Pillared Aluminum Ethylene Diphosphonate Displaying Reversible Dehydration−Rehydration Behavior." *Chemistry of Materials* 16.11 (**2004**): 2229-237.

32. Reddy, B., Krishna K.; Rao, K. P.; Vidyasagar, K, Syntheses, structure and intercalation properties of low-dimensional phenylarsonates, A(HO3AsC6H5)(H2O3AsC6H5) (A = Tl, Na, K and Rb), *European Journal of Inorganic Chemistry*, **2006**, 4, 813-819

33. Chen, B.; Zapata, F.; Fronczek, F. R>; Lobkovsky, E. B.; Zhou, H. C., Rationally Designed Micropores within a Metal−Organic Framework for Selective Sorption of Gas Molecules, *Inorg. Chem.,* 2007, 46, 1233.

34. Riyad R. Irani K. M., Metal complexing by phosphorus. VI. Acidity constants and calcium and magnesium complexing by mono- and poly methylene diphosphonates, *J. Phys. Chem.*, **1962**, *66* (7), pp 1349–1353

35. Serre, C.; Ferey, G. Hydrothermal Synthesis and Structure Determination from Powder Data of New Three-Dimensional Titanium(IV) Diphosphonates $Ti(O_3P-(CH_2)_n-PO_3)$ or MIL-25$_n$ ($n$ = 2, 3), *Inorganic Chemistry*, **2001**, 40, 5350-5353

36. Merrill, C. A.; Cheetham, A. K. Pillared Layered Structures Based upon M(III) Ethylene Diphosphonates:□ The Synthesis and Crystal Structures of $M^{III}(H_2O)(HO_3P(CH_2)_2PO_3)$ (M = Fe, Al, Ga), *Inorganic Chemistry*, **2005**, 44, 5273-5277

37. Schmidt, M. U.; Schmiermund T.; Bolte M., Anilic acid dimethylformamide disolvate, Acta Crystallographica, **2007**, E63, m360-m362

38. Cabeza, A.; Aranda, M. A. G.; Bruque, S.; Poojary, D. M.; Clearfield, A, Synthesis, ab initio structure determination, and characterization of manganese(III) phenyl phosphonates, Progress in inorganic chemistry, **1998**, 47, 371-374

39. Serpaggi F. and Férey G., Hybrid open frameworks (MIL-n). Part 6 Hydrothermal synthesis and X-ray powder ab initio structure determination of MIL-11, a series of lanthanide organodiphosphonates with three-dimensional networks, $Ln^{III}H[O_3P(CH_2)_nPO_3]$ (n=1-3), *J. Mater. Chem.*, **1998**, 8, pg 2749-2755

40. Petrucci, H., Herring, M., General Chemistry: Principles & Modern Applications, Ninth Ed. Upper Saddle River, NJ: Pearson Education, Inc., **2007**.

41. Sasse K., *Houben-Weyl* **12/1,** 433 (1963); B. A. Arbuzov, *Pure Appl. Chem.* **9,** 307 (1964); G. M. Kosolapoff, *Org. React.* **6,** 276 (1951); D.

Redmore, *Chem. Rev.* **71,** 317 (1971); G. Bauer, G. Haegele, *Angew. Chem. Int. Ed.* **16,** 477 (1977); A. K. Bhattacharya, G. Thyagarajan, *Chem. Rev.* **81,** 415 (1981); B. Faure *et al., Chem. Commun.* **1989,** 805; V. K. Yadav, *Synth. Commun.* **20,** 239 (1990).

42. Zumdahl, S. S., and Zumdahl S. A., *Chemistry*. Boston: Houghton Mifflin, 2007.

43. Laudise, R.A., Doremus, R.H., Roberts, B.W. and Turnbull, D., *Growth a nd perfection of crystals. Prroceedings of an International Conference on Crystal Growth held at Cooperstown, New York on August 27–29, 1958.* Wiley, New York. pp. 458–463.

44. Malachowski M. R., Dorsey B., Sackett G. J., Kelly R. S. Ferko A. L., R. N. Hardin, Effect of ligand donors on the catalytic properties of metal complexes. Copper(R) complexes as catalysts for the oxidation of 3,5-di-tert-butylcatechol, Chemistry Department of San Diego university, **1995**

# SUMMARY

The skeletal system plays a significant role allowing for movement and other essential functions. There are many causes such as diseases resulting in deformity and malfunctions. However bone has the ability to regenerate allowing it to heal over a period of time when it is damaged. The repairing process occurs in multiple steps. Thus, the main focus of this project was to seek a way to enhance the healing process by introducing a biocompatible scaffold. The use of scaffolds is common in biology to enhance the growth of new cells so the same concept was applied to bones in repair process. Scaffolds are based on biocompatible magnesium and calcium alkaline earth metals based diphosphonates. Magnesium and calcium are often found in most of our body system.

The ligand system used is derived from the use of diphosphonate based drugs in bone therapy. There are various kinds of diphosphonate based drugs available in the market and they are used to reduce pain, reduce bone fracture and prevent the progress of tumor growth in bone related disorders such as osteoporosis, Paget's disease, bone metastases, and hypercalcemia. While exogenous phosphonic acids are known to bind to calcium in the bone, diphosphonates are also known as agents for suppressing resorption of bone.

Preferably the targeted scaffolds contain pores to allow the incorporation of fluids and substances. Similar characteristics are found in metal organic frameworks (MOFs) which provide a model system for the targeted material.

MOFs are crystalline compounds consisting of metal ions or clusters coordinated to often rigid organic molecules to form 1-, 2-, 3-dimensional structures which maybe porous. MOFs are usually robust, rigid and thermally stable. They have formed used in a wide range of applications. A significant drawback is the difficulty to control and to predict the characteristics of each MOF. However, the focus is to produce MOFs that are 3-dimensional containing pores.

The ligand, 3-oxapentane-1,5-diphosphonic acid, choice is based on the special properties and binding modes it may have compared to previously used ligands such as ethylene diphosphonic acid and butylenes diphosphonic acid. Hence, I expect to see different products that will exhibit different coordination and aggregation characteristics. Nevertheless, the most significant characteristic many researchers focus is on the size of pores.

Transition metal phosphonates and diphosphonates have been widely disseminated; however analogous $s$-block metal complexes are rare. A multitude of factors contribute towards this. A range of significant differences between the two groups of metals is apparent, including the larger size of the $s$-block metals. The large size of the $s$-block metals results in large coordination numbers and a pronounced tendency towards aggregation. The absence of energetically available

d-orbital for the *s*-block metals, along with the electropositive characters for the *s*-block metals result in mainly electrostatic bonds and s-orbital control.

This project employed the well-known Michaelis-Arbuzov reaction to prepare the target ligand. A new synthetic route for the synthesis of diphosphonate ligand was established. The ligand was treated with different calcium and magnesium salts using different pH, temperature, solvent and pressure conditions affording solid products for three different reactions conducted. In order to obtain crystals with high quality hydrothermal reaction was employed in this project. Hydrothermal synthesis is based on the increased solubility of reagents and products under high pressure and high temperature conditions. The improved solubility will facilitate crystal growth. Unfortunately, the crystal quality did not allow their characterization with single crystal X-ray crystallography.

Three compounds were characterized with three alternative methods, melting point, IR spectroscopy, and ^{1}H-NMR. ^{1}H-NMR indicated slight changes in chemical shifts and this is quite important because the metal coordination influences the protons in compound when they interact with a part of a compound which leads to the changes in the chemical shift observed in the ^{1}H NMR. In addition, IR spectroscopy have shown changes in finger print area and this is also important because each compounds have their own distinct peaks in this area just like how we have our own distinct finger prints. Lastly, melting point tests have given a strong indication of the product formation. All three compounds had

different melting points and slight shifts in $^1$H NMR spectra as compared to the starting materials, indicating that some chemical changes must have occurred during the hydrothermal reaction.

In summary, a new synthetic route to synthesize the ligand is established and three products have been formed although the quality prevented from producing details of crystallographic data and structure refinement parameters.

However, the results of this project have shown the need of further studies with corresponding chemistry. Future work will include the further exploration of reaction conditions and crystallization methods, including the addition of lewis bases, as well as other magnesium and calcium salts.